Comparison of Linearized Electrical Degradation Kinetics in Metal-Activated Spinel $(Cu,Ni,Co,Mn)_3O_4$ Ceramics–Matrix Nanocomposites

V. Balitska[a,*], O. Shpotyuk[b,c] and M. Brunner[d]

[a]Lviv State University of Life Safety, 35, Kleparivska Str., Lviv, 79007, Ukraine

[b]Jan Długosz University in Częstochowa, al. Armii Krajowej 13/15, 42-200 Częstochowa, Poland

[c]Vlokh Institute of Physical Optics, 23, Dragomanov Str., Lviv, 79005, Ukraine

[d]Technische Hochschule Köln/University of Technology, Arts, Sciences, 2, Betzdorfer Str., Köln, 50679, Germany

(Received April 2, 2019; revised version February 11, 2020; in final form February 11, 2020)

Phenomenological models of degradation kinetics are considered for jammed systems like inhomogeneous ceramics–matrix nanocomposites, which are exemplified, in part, by screen-printed $Cu_{0.1}Ni_{0.1}Co_{1.6}Mn_{1.2}O_4$ spinel ceramics with conductive Ag and Ag–Pd contacting alloys. Structurally-intrinsic inhomogeneities due to Ag or Ag–Pd diffusants in spinel ceramics environment are shown to define governing kinetics of thermally-induced electrical degradation at 170 °C, obeying an obvious non-exponential behaviour in negative relative resistance drift. Numerical parametrization of this phenomenon (in part, determination of kinetics-responsible scaling exponent β) can be simply performed within indirect linear least-square analysis applied to generalized relaxation function presented in the double-logarithmic plot of variables. Crossover from stretched-exponential ($0 < \beta < 1$) to compressed-exponential ($\beta > 1$) degradation kinetics is revealed in these nanocomposites depending on the contacting diffusants, i.e., conductive Ag–Pd ($\beta = 0.58$) or Ag ($\beta = 1.68$) compounds.

DOI: 10.12693/APhysPolA.137.1027

PACS/topics: 81.05.Je

1. Introduction

A great variety of metastable solid substances, rapidly quenched from disordered far-from-equilibrium liquid state, possesses internal stresses inevitably, which is built in at a so-called jamming fluid-to-solid transition [1, 2]. Typical examples of such jammed systems include different structurally-inhomogeneous nanocomposites like foams and soft glasses, dense colloidal fractal gels (soft glassy and lamellar gels), micellar polycrystals, concentrated emulsions, clay suspensions (colloidal glass and clays), polymer–matrix composites, nanoparticle-filled super-cooled liquids and glassy polymer melts, polymer composites disturbed by internal stresses, many kinds of metallic vitreous alloys (like $Mg_{65}Cu_{25}Y_{10}$, or $Zn_{67}Ni_{33}$), etc. [1–12]. Many of these out-off-equilibrium solid-state systems realize their functionality due to internal structural inhomogeneities frozen at atomic and/or sub-atomic length scales, which modify their physical-chemical properties and materials' response to different external activations. With tendency towards equilibrium for the controlled parameter $N_\eta(t)$, such systems obey non-usual relaxation kinetics, which can be specifically distinguished as compressed-exponential relaxation (CER) kinetics (alternatively also termed as super-exponential or squeezed-exponential):

$$N_\eta(t) \sim \exp\left(\left(-\frac{t}{\tau}\right)^\beta\right), \tag{1}$$

described by compressing exponent $\beta > 1$ and characteristic time τ (dependent on the scattering vector q as q^{-1}, instead of q^{-2} behaviour in conventional thermally activated diffusion [1, 2]). This is faster than simple exponential decay (SED) kinetics with $\beta = 1$:

$$N_\eta(t) \sim \exp\left(-\frac{t}{\tau}\right). \tag{2}$$

This unusual anomalous dynamics in structurally-inhomogeneous systems is explained in terms of ultraslow ballistic motion of intrinsic scatters (carriers of ballistic-like motion) under internal stress frozen at a so-called jamming transition [1]. The built-in stress fields are frozen around some inhomogeneities (such as agglomerates of embedded nanoparticles, atomic clusters, absorbed molecules, etc.) to counter reduction in an entropy due to interaction with the surrounding. The compressing exponent β in Eq. (1) serves as a measure of these internal stresses developed in such jammed systems under their tendency towards metastable state. Conversely, the collapse of internal stresses in more equilibrium thermodynamic conditions approaching a super-cooled liquid state causes substantial changes in the underlying degradation kinetics, which attains SED functional (2) with $\beta = 1$.

This CER-to-SED crossover is well realized in soft jammed systems, where carriers of diffusive-like motion prevails (β=1), such as super-cooled liquid-like polymers filled with "hard" filler nanoparticles (diffusants) [3–6].

*corresponding author; e-mail: vbalitska@yahoo.com

In its preferential occurrence, this CER-to-SED crossover seems to be thermally activated, being realized near glass transition temperature T_g and showing hyper-diffusive behaviour (viz. CER) at low temperatures ($T < T_g$) and SED dynamics at high temperatures ($T > T_g$).

More specifically, in many structurally-dispersive systems, wide variety of characteristic times τ changes the degradation kinetics to stretched-exponential relaxation (SER) with $0 < \beta < 1$ (sub-exponential relaxation), which is slower than SED kinetics determined by Eq. (2). As a result, the temperature variation over out-of-equilibrium (glassy-like) and close-to-equilibrium (super-cooled-liquid) states is hallmarked in universal dynamical thermally-activated CER-to-SER kinetics crossover, as it occurs, e.g., in different types of metallic glasses [7, 8]. Alternatively, the degradation kinetics walking over these metastable glassy-like and super-cooled liquid states can be traced via physical ageing (the process of the system evolution from as-prepared rejuvenated to more relaxed equilibrium state [8]), as it is a characteristic for colloidal suspensions of laponite [9–12]. Thus, spontaneously aged colloidal suspensions were characterized by SER kinetics with $\beta < 1$ (varying around 0.5–0.8 depending on waiting times t), while CER behaviour with $\beta > 1$ (varying around ≈ 1.5 in depending on t) was found for the same rejuvenated samples [9].

Thereby, at a global scale, we can balance over these ageing-induced and thermally-activated CER-to-SER crossovers, by describing both types of non-exponential kinetics using the above Eq. (1) as a unified master equation with scaling exponent β (viz. non-exponentionality index) attaining all positive β values, i.e., $0 < \beta < 1$ for stretching (SER) and $\beta > 1$ for compressing (CER) dependences.

Parametrization of this generalized approach describing degradation kinetics by Eq. (1) can be simply linearized in the double-logarithmic plotting of variables

$$\ln\left(-\ln N_\eta\left(t\right)\right) \sim \beta \ln t - \beta \ln \tau. \tag{3}$$

In this linear presentation (3), both parameters (the scaling exponent β and characteristic time τ) are reliably defined from the straight line $y = \ln(-\ln N_\eta(t)) = f(\ln t)$, by employing a least-square fitting procedure as it was performed, e.g., in Ref. [13] to visualize non-exponential stress relaxation in some chalcogenide glasses.

In this work, we apply the above linearization approach to analyze other representative of this CER-to-SER kinetics crossover, which is revealed in thermally-induced electrical degradation in screen-printed structures of spinel-type $(Cu,Ni,Co,Mn)_3O_4$ manganites with different metallic diffusants, which are Ag- and Ag–Pd conducting compounds (the case of diffusant-dependent CER-to-SER kinetics crossover [14]).

2. Materials and methods

The degradation tests were performed with spinel $Cu_{0.1}Ni_{0.1}Co_{1.6}Mn_{1.2}O_4$ thick films prepared by screen-printing as described in more detail elsewhere [14–18]. The starting ceramics were sintered (at 1040 °C) using carbonate hydroxides and hydrates of the corresponding transition metals [19–21]. The paste was prepared by mixing the powdered $Cu_{0.1}Ni_{0.1}Co_{1.6}Mn_{1.2}O_4$ spinel ceramics with MB-60 glass, Bi_2O_3 binder, and some organic vehicle. Then, the paste was printed on alumina substrates (Rubalit 708S) with conductive Ag- or Ag–Pd layer (preliminary printed from C1216 paste). Finally, these structures were fired at 850 °C. The prepared thick-film spinel-metallic composites were subjected to degradation tests at 170 °C by subsequent cycling (during 24–360 h). The confidence interval in the relative resistance drift (RRD), e.g. changes in electrical resistance $\Delta R/R_0$ of these structures measured under normal conditions, were not worse than ±0.2%, and overall uncertainties in RRD measurements did not exceed ±0.5%.

For adequate phenomenological description of the observed thermally-induced degradation kinetics, the experimental $\Delta R/R_0$ values were treated by direct non-linear least-square curve fitting to the generalized relaxation function presented as [22, 23]:

$$N\eta(t) = \mathrm{RRD} = a\left[\exp\left(-\left(\frac{t}{\tau}\right)^{\beta}\right) - 1\right], \tag{4}$$

where a stands for amplitude, τ is time constant, and β is non-exponentionality index. Numerical values of a, τ, and β parameters used in above Eq. (4) were calculated in a way to minimize the mean-square deviations err of the experimental points from the model curve. These parameters were also extracted from indirect linear least-square curve fitting using linearized double-logarithmic functional (3). Under known uncertainties in $\Delta R/R_0$ values, the estimated accuracy in β was ±0.05.

3. Results and discussion

The typical kinetics curves illustrating normalized RRD values defined as $\Delta R/R_0 = N_\eta(t)$ with respect to Eq. (4) in $Cu_{0.1}Ni_{0.1}Co_{1.6}Mn_{1.2}O_4$ ceramics with screen-printed contacts prepared of Ag or Ag–Pd compounds are depicted in Fig. 1. It is obvious that degradation kinetics essentially differ in their general occurrence for these cases. Indeed, the films with Ag–Pd contacts demonstrate sharp decreasing trend in the $N_\eta(t)$ with waiting time t ending by prolonged saturation at $t > 200$ h, thus obeying characteristic SER shape with non-exponentionality index β approaching ~ 0.58 and time constant $\tau \cong 32$ h. Numerical values of both parameters were obtained by direct non-linear least-square analysis of tested kinetics using Eq. (4).

With change in the diffusant material on metallic Ag (under transition to ceramics–Ag nanosystem), the initial decreasing trend in the control parameter $N_\eta(t)$ is evidently suppressed, being more stretched over shorter time periods $t < 30$–40 h. Then, this kinetics attain sharper decay, resulting in saturation at longer waiting times $t > 250$–300 h. Thereby, the governing kinetics are drastically changed in this case, attaining an obvious

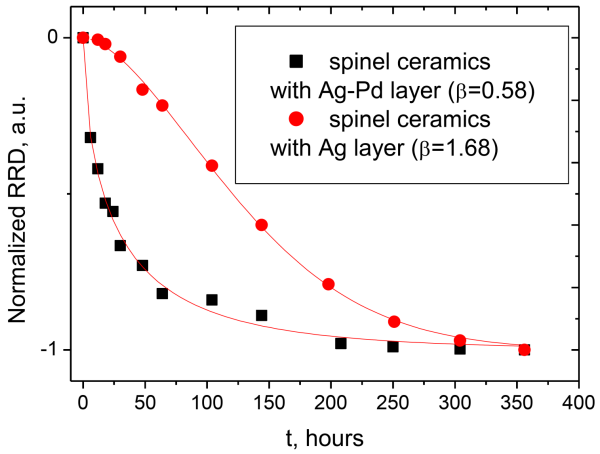

Fig. 1. Normalized kinetics of thermally-induced (170 °C) degradation revealed by RRD $= \Delta R/R_0 = N_\eta(t)$ in thick-film spinel $Cu_{0.1}Ni_{0.1}Co_{1.6}Mn_{1.2}O_4$ ceramics with screen-printed Ag–Pd (black squares) and Ag (red circles) contacting layers.

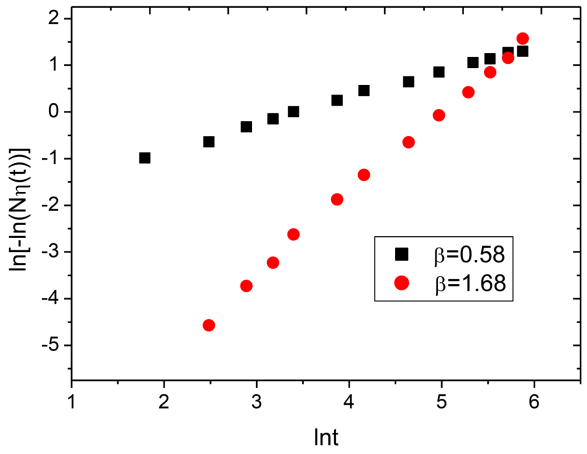

Fig. 2. Comparative double-logarithmic presentation of the linearized kinetics of thermally-induced (170 °C) degradation revealed by RRD $= \Delta R/R_0 = N_\eta(t)$ in thick-film spinel $Cu_{0.1}Ni_{0.1}Co_{1.6}Mn_{1.2}O_4$ ceramics with screen-printed Ag–Pd (black squares) and Ag (red circles) contacting layers.

sigmoidal shape for CER curve [24] with fitting parameters β and τ (the over-unity compressibility index $\beta = 1.68$ and $\tau \cong 154$ h).

In Fig. 2, electrical degradation kinetics for screen-printed structures with Ag and Ag–Pd contacts are shown in linearized double-logarithmic presentation of Eq. (3). Both β and τ parameters can be extracted from indirect linear least-squares analysis as respective slope tangent and starting coordinate of $y = \ln(-\ln N_\eta(t)) = f(\ln t)$ straight lines (see Fig. 2). This procedure allows reliable determination of $\beta = 0.58$ and $\tau = 32.5$ h for film with Ag–Pd contacts, and $\beta = 1.68$ and $\tau = 155.6$ h for film with Ag contacts.

Conductive material penetrating spinel ceramics is known to reduce its electrical resistivity resulting in negative RRD [17, 25, 26]. This diffusive process is thermally activated, in contrast to its own changes, producing positive feedback in RRD due to increased defectiveness of ceramics [27]. The diffusive process quickly saturates with conductive material penetrating into ceramics as it is a characteristic for $Cu_{0.1}Ni_{0.1}Co_{1.6}Mn_{1.2}O_4$ film with Ag–Pd contacts, which behaves as one "cumulative" diffusing agent with a significantly suppressed possibility for Ag atoms migration. The resulting kinetics of such diffusive degradation attains strong tendency to yield SER scenarios, as it is illustrated by non-linear least-squares curve fitting in Fig. 1 (black points) or indirect linear least-squares curve fitting in Fig. 2.

However, if Ag penetration is not inhibited in ceramics owing to compounding with Pd (as for $Cu_{0.1}Ni_{0.1}Co_{1.6}Mn_{1.2}O_4$ thick film with contacts made of screen-printed Ag paste), the resulting electrical relaxation kinetics is changed essentially. The Ag atoms can migrate in spaces between crystalline grains filled with glass binder. This single-stage diffusion-related process quickly saturates via SER dependence (1) obeying the scaling exponent $0 < \beta < 1$.

In terms of heterogeneity [28], the observed non-exponential kinetics can be described by heterogeneity factor h (the inverse $1/\beta$ value), quantifying system deviation from simple SED kinetics (2). In our case, this parameter for SER kinetics is greater ($h = 1.72$), reflecting complex glassy process dominated by multiple local minima, while for CER kinetics $h = 0.6$, due to non-exponential kinetics in Ag penetrating $Cu_{0.1}Ni_{0.1}Co_{1.6}Mn_{1.2}O_4$ ceramics. It should be admitted reasonably that Ag atoms penetrating spinel-type ceramics, mainly in a vicinity of intergranual boundaries, create specific micron-sized bridges between ceramics grains. This increases electrical conductivity of whole ceramics–matrix composite.

In fact, transition to CER kinetics in $Cu_{0.1}Ni_{0.1}Co_{1.6}Mn_{1.2}O_4$ nanocomposite with Ag layer is caused by enhanced penetration ability of this metallic activator in ceramics matrix. The similar non-exponentionality index β was also observed in many soft out-of-equilibrium systems such as fractal colloidal gels with $\beta \cong 1.5$ ascribed to deformations of elastic network due to the syneresis of the gels [29, 30]. In concentrated emulsions and lamellar gels (also with with $\beta \cong 1.5$), the driving microstructure mechanism responsible for CER kinetics is collapse of heterogeneous initial distribution of stresses due to soft contacts between near-spherical particles or local topological rearrangements [31]. In micellar polycrystals with $\beta \cong 1.3$–1.7 [31], the CER behaviour observed in dynamic structure factor is attributed to rearrangement of polycrystal texture, i.e., elastic relaxation of topological defects like dislocations and/or grain boundaries. The CER kinetics was also detected in many hard out-of-equilibrium systems such as metallic glasses [32, 33], where it was ascribed to ballistic-like hopping motion due to stress relaxation.

In many polymer-matrix nanocomposites such as PMMA capped Au [5] or Al_2O_3 particles [6] with scaling exponent β approaching 1.4–1.9 (depending on nanoparticle content), the CER kinetics appear at lowering temperature below the glass transition temperature (thus producing thermally-activated CER-to-SER kinetics crossover). In many rejuvenated colloidal glasses [9–12], the similar CER-to-SER crossover can be activated under physical ageing (thus producing aging-induced CER-to-SER kinetics crossover). It should be noted that the same order of β (serving as a measure of internal stress), defined by diffusant-dependent SER-to-CER kinetics crossover for thermally-relaxing nanocomposite systems in photo-switchable folded α-helix [34], rejuvenated colloidal glasses [9–12], or polymer nanocomposites [5, 6], testifies in favour of phenomenological similarity in responsible models.

4. Conclusions

Principally different types of non-exponential degradation kinetics are studied for the same thick-film spinel $Cu_{0.1}Ni_{0.1}Co_{1.6}Mn_{1.2}O_4$ ceramics–matrix nanocomposite in dependence on contacting diffusants (Ag or Ag–Pd alloys). If Ag migration is inhibited in $Cu_{0.1}Ni_{0.1}Co_{1.6}Mn_{1.2}O_4$ ceramics due to compounding with Pd as for Ag–Pd alloy, the governing kinetics attains a stretched exponential behaviour with scaling exponent $\beta \sim 0.58$, which is characteristic for one-stage diffusion in dispersive media. Under Ag penetration deeply into ceramics body, as is the case for spinel ceramics with Ag contacts, the kinetics drastically changed, attaining compressed-exponential behaviour with over-unity scaling exponent β approaching ~ 1.68. The observed diffusant-dependent CER-to-SER kinetics crossover can be simply parametrized employing indirect linear least-squares analysis applied to the generalized relaxation function in double-logarithmic plot of variables.

References

[1] L. Cipelletti, L. Ramos, S. Manley, E. Pitard, D.A. Weitz, E.E. Pashkovski, M. Johansson, *Faraday Discuss.* **123**, 237 (2003).

[2] L. Cipelletti, S. Manley, R.C. Ball, D.A. Weitz, *Phys. Rev. Lett.* **84**, 2275 (2000).

[3] H. Guo, G. Bourret, M.K. Corbierre et al., *Phys. Rev. Lett.* **102**, 075702-1 (2009).

[4] C. Caronna, Y. Chushkin, A. Madsen, A. Cupane, *Phys. Rev. Lett.* **100**, 055702-1 (2008).

[5] S. Srivastava, A.K. Kandar, J.K. Basu, M.K. Mukhopathyay, L.B. Lurio, S. Narayanan, S.K. Sinha, *Phys. Rev. E* **79**, 021408-1 (2009).

[6] R.A. Narayanan, P. Thiyagarajan, S. Lewis, A. Bansal, L.S. Schadler, L.B. Lurio, *Phys. Rev. Lett.* **97**, 075505-1 (2005).

[7] B. Ruta, G. Baldi, G. Monaco, Y. Chushkin, *J. Chem. Phys.* **138**, 054508-1 (2013).

[8] B. Ruta, Y. Chushkin, G. Monaco, L. Cipelletti, E. Pineda, P. Bruna, V.M. Giordano, M. Gonzalez-Silveira, *Phys. Rev. Lett.* **109**, 165701-1 (2013).

[9] R. Angelini, L. Zulian, A. Fluerasu, A. Madsen, G. Ruocco, B. Ruzicka, *Soft Matter* **9**, 10955 (2013).

[10] R. Angelini, A. Madsen, A. Fluerasu, G. Ruocco, B. Ruzicka, *Coll. Surf. A* **460**, 118 (2014).

[11] R. Angelini, E. Zaccarelli, F. Augusto, M. Marques, M. Sztucki, A. Fluerasu, G. Ruocco, B. Ruzicka, *Nature Commun.* **5**, 4009-1 (2014).

[12] R. Angelini, B. Ruzicka, *Coll. Surf. A* **483**, 316 (2015).

[13] Y. Gueguen, V. Keryvin, T. Rouxel, M. Le Fur, H. Orain, B. Bureau, C. Boussard-Pledel, J.-C. Sangleboeuf, *Mech. Mater.* **85**, 47 (2015).

[14] V. Balitska, O. Shpotyuk, M. Brunner, I. Hadzaman, *Chem. Phys.* **501**, 121 (2018).

[15] I. Hadzaman, H. Klym, O. Shpotyuk, *Int. J. Nanotechnol.* **11**, 843 (2014).

[16] H. Klym, I. Hadzaman, O. Shpotyuk, *Can. J. Phys.* **92**, 822 (2014).

[17] H. Klym, V. Balitska, O. Shpotyuk, I. Hadzaman, *Microelectron. Reliabil.* **54**, 2843 (2014).

[18] H. Altenburg, J. Plewa, G. Plesch, O. Shpotyuk, *Pure Appl. Chem.* **74**, 2021 (2002).

[19] M. Vakiv, O. Shpotyuk, O. Mrooz, I. Hadzaman, *J. Eur. Ceram. Soc.* **21**, 1783 (2001).

[20] O. Bodak, L. Akselrud, P. Demchenko et al., *J. Alloys Compd.* **347**, 14 (2002).

[21] O. Shpotyuk, V. Balitska, I. Hadzaman, H. Klym, *J. Alloys Compd.* **509**, 447 (2011).

[22] O. Shpotyuk, M. Brunner, I. Hadzaman, V. Balitska, H. Klym, *Nanoscale Res. Lett.* **11**, 499-1 (2016).

[23] O. Shpotyuk, V. Balitska, M. Brunner, *J. Phys. Conf. Ser.* **936**, 012050-1 (2017).

[24] D. Hamada, C.M. Dobson, *Protein Sci.* **11**, 2417 (2002).

[25] V. Balitska, O. Shpotyuk, *Archiv. Mater. Sci.* **27**, 189 (2006).

[26] V. Balitska, O. Shpotyuk, H. Klym, J. Plewa, H. Altenburg, in: *Proc. 1st ECErS Conf.*, Eds. J.G. Heinrich, C. Aneziris, Göller Verlag, Baden-Baden 2007, p. 837.

[27] M.M. Vakiv, O.I. Shpotyuk, V.O. Balitska, B. Butkiewicz, L.I. Shpotyuk, *J. Eur. Ceram. Soc.* **24**, 1243 (2004).

[28] B. Gillespie, K.W. Plaxco, *PNAS* **97**, 12014 (2000).

[29] E.S. Matsuo, T. Tanaka, *Nature* **358**, 482 (1992).

[30] C. Hashimoto, H. Ushiki, *Polym. J.* **32**, 807 (2000).

[31] E.S. Matsuo, T. Tanaka, *J. Chem. Phys.* **89**, 1695 (1988).

[32] C. Hashimoto, P. Panizza, J. Rouch, H. Ushiki, *J. Phys. Condens. Matter* **17**, 6319 (2005).

[33] C. Hashimoto, P. Panizza, J. Rouch, H. Ushiki, *J. Chem. Phys.* **124**, 044903-1 (2006).

[34] R. Hamm, J. Helbing, J. Bredenbeck, *Chem. Phys.* **323**, 54 (2006).